Laboratory exercises to study viscous boundary layers in the test section of an open-circuit wind tunnel

Josué Njock Libii

Indiana University-Purdue University Fort Wayne
Fort Wayne, Indiana, United States of America

ABSTRACT: Laboratory exercises presented here were designed and tested in the fluid mechanics laboratory so as to study viscous boundary layers in the test section of an open-circuit wind tunnel. These exercises create hands-on learning opportunities through which students gain practical experience with the highly abstract concepts of viscous boundary layers. They yield results very close to those in the published literature. The introduction reviews the concepts of thicknesses of the viscous boundary layer over a flat plate with zero pressure gradient when the boundary layer is laminar and when it is turbulent. Lab exercise 1 shows how to use a wind tunnel to determine the speed of the air through its test section. Lab exercise 2 shows how students can measure boundary-layer thicknesses in the test section of the wind tunnel. Results compare very well with those from boundary-layer theory.

INTRODUCTION

Consider flow over a flat plate with a zero pressure gradient. When the flow is such that its boundary layer is laminar, the exact solution proposed by Blasius gives the thickness of the boundary layer along the plate [1]. The relation is [2][3]:

$$\delta(x) = \frac{5.0x}{\sqrt{\mathrm{Re}_x}} \tag{1}$$

with

$$\mathrm{Re}_x = \frac{Ux}{\nu}. \tag{2}$$

Where x is the distance along the flat plate measured from the leading edge; δ is the thickness of the boundary layer at a point of coordinate x; U is the free stream speed of the air; ν is the kinematic viscosity of the air; and Re_x is the Reynolds number in which one uses the distance x as a characteristic length.

When the boundary layer is turbulent, its thickness cannot be determined exactly. However, it can be estimated by using the momentum-integral equation given by:

$$\frac{\tau_w}{\rho} = \frac{d}{dx}\left(U^2\theta\right) + \delta^* U \frac{dU}{dx} \tag{3}$$

together with the assumption that u, the speed of air inside the boundary layer, follows a power-law profile given by:

$$\frac{u}{U} = \left(\frac{y}{\delta}\right)^{1/n}, \tag{4}$$

$$\frac{\overline{V}}{U} \equiv \frac{2n^2}{(n+1)(2n+1)} = \alpha$$

where τ_w is the wall shear stress, ρ the mass density of the fluid, x is the distance along the plate that is measured from the leading edge, U is the centreline velocity in a power-law velocity distribution; here, it will be taken as the

free-stream speed; $\overline{V}$ is the average velocity, α is the ratio of the average velocity to the centreline velocity, θ is the momentum thickness, δ^* is the displacement thickness, δ is the boundary-layer thickness at x, and y is the distance from the flat plate. The momentum thickness and the displacement thickness are defined, respectively, by

$$\theta = \int_0^{\infty} \frac{u}{U}\left(1-\frac{u}{U}\right)dy \approx \int_0^{\delta} \frac{u}{U}\left(1-\frac{u}{U}\right)dy \tag{5}$$

and

$$\delta^* = \int_0^{\infty}\left(1-\frac{u}{U}\right)dy \approx \int_0^{\delta}\left(1-\frac{u}{U}\right)dy \tag{6}$$

Integration of Eq. (4) in the momentum-integral equation shows that the thickness of the boundary layer is given by

$$\delta(x) \cong \frac{ax}{\left(\mathrm{Re}_x\right)^{1/5}}; \tag{7}$$

where

$$a = a(n) \tag{8}$$

It can be seen that *a(n)* is a function of n only. Carrying out the necessary algebra, one gets:

$$a = 0.07842\left\{\frac{\left[\frac{2n^2}{(n+1)(2n+1)}\right]^{7/5}}{\left(\frac{n}{2+3n+n^2}\right)^{4/5}}\right\} \tag{9}$$

Thus, for a given *n*, the numerical value of *a* can be determined. The results of the process of determining *a* for various values of *n* are shown in Table 1 below.

Table 1: Turbulent boundary layer over a flat plate at zero incidence: results.

$\frac{u}{U} = \eta^{1/n}$	$\frac{\theta}{\delta}$	$\frac{\delta^*}{\delta}$	$H = \frac{\delta^*}{\theta}$	$a \equiv \frac{\delta}{x}\left(\mathrm{Re}_x\right)^{1/5}$	$b = C_f\left(\mathrm{Re}_x\right)^{1/5}$
$\eta^{1/6}$	0.107143	0.142857	1. 333333	0.337345906	0.057830727
$\eta^{1/7}$	0.097222	0.125	1.285714	0.381143751	0.059289028
$\eta^{1/8}$	0.088889	0.111111	1.250000	0.423532215	0.060235693
$\eta^{1/9}$	0.0818181	0.10000	1.222222	0.464755563	0.060840728
$\eta^{1/10}$	0.0757575	0.9090909	1.200000	0.504990077	0.061210918
…	…	…	…	…	…

A similar table for laminar boundary layers is given by Fox and McDonald [2]. From Table 1, it can be seen that the boundary-layer thickness, δ, is larger than both the momentum thickness, θ, and the displacement thickness, δ^*. However, the displacement thickness, δ^*, is larger than the momentum thickness, θ. This Table was used to study boundary layers in the test section of a closed-circuit wind tunnel. This is illustrated in lab exercise 2.

The remainder of the article is organised in the following way: First, the wind tunnel used in experiments is described; next, an experiment that shows how to calibrate a wind tunnel is presented. Then, an experiment that demonstrates the existence of the boundary layer is presented. Finally, the results of the second experiment are analysed using standard boundary-layer theory to characterise the nature of boundary layers in the test section of the wind tunnel for the air speeds used during testing.

THE WIND TUNNEL USED

An open-circuit Eiffel wind tunnel Model 402 B made by Engineering Laboratory Design, Inc., was used [4]. It has a velocity range of 3.0–48.7 m/s (10.0 – 160fps); its test section has a vertical cross section of 30.5 cm x 30.5 cm (12 in x 12 in), a length of 61.0 cm (24 in), and it is equipped with a 7.5 kW (10.0 HP) motor (Figure 1). Different parts of the wind tunnel are identified and labelled in Figure 2.

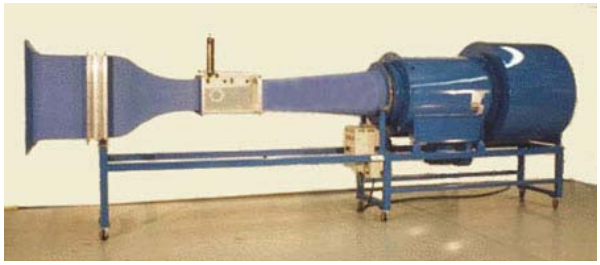

Figure 1: Open-circuit Eiffel wind tunnel Model 402 B by ELDINC [4].

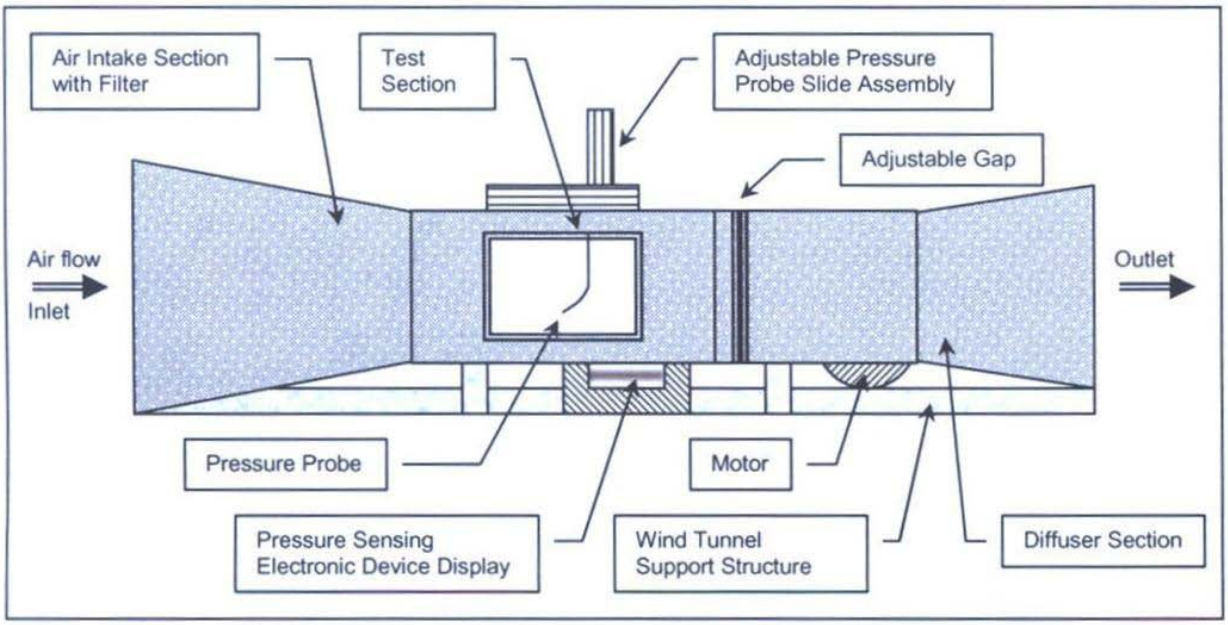

Figure 2: Parts of the wind tunnel used in experiments (Courtesy of J.J. Thomas).

EXPERIMENT 1: CALIBRATION OF A WIND TUNNEL

The purpose of this experiment is threefold: 1) students learn how to use the settings of the wind tunnel to achieve a desired wind speed; 2) they practise how to apply this knowledge to determine the full range of speeds attainable in the wind tunnel being used; and 3) they use collected data to plot a calibration curve that relates the wind speed in the test section to the sizes of the adjustable gap between the intake and the outlet sections of the tunnel (Figure 2).

Wind tunnels ordinarily have mechanisms to change the speed of the air in them. ELD's model 402 B used in this experiment achieves this by changing the length of the tunnel. This is done by creating an air gap between the exit end of the tunnel, where the fan is located, and its inlet end, where the test section is located. The width of the gap so created can be measured and each setting of the gap corresponds to a specific speed of air in the wind tunnel. By changing the width of this gap progressively in specified increments, and measuring the air speed at each step, one generates a table of air speeds corresponding to the gap openings tested. Instrumentation available in the wind tunnel allows the experimenter to read the difference between the stagnation and static pressures at a selected point inside the test section for each gap opening. Using Bernoulli's equation for steady, inviscid, and incompressible flows, this difference in pressures can be converted into the average speed at the selected point by means of Equation (10):

$$V = \sqrt{\frac{2(p_0 - p)}{\rho}} \tag{10}$$

where V is the speed of the moving air, p_0 is the stagnation, or total, pressure, p is the static pressure at the specified point, and ρ is the mass density of the air in the test section. For air, the ideal-gas law can be used to compute the mass density of air for the temperature and pressure in the laboratory. Alternatively, such a mass density can be obtained by looking it up in appropriate tables.

For ELD's wind tunnel model 402 B, the differences between the stagnation and static pressures in the test section were measured for each tested gap size. The measurements were obtained by carrying out the procedure described above repeatedly. The corresponding calibration curve, that is, the plot of air speed as a function of the size of the gap, is shown in Figure 3 [5].

It can be seen from Figure 3 that the speed of air in the test section decreases, as one increases the size of the gap. This is as expected, and here is the explanation: when the gap is completely closed, all the flow energy provided by the spinning fan blades goes into moving air from the open lab spaces into the inlet of the wind tunnel, through the test section, and out the outlet. In this case, there is only one inlet port to the tunnel and only one outlet port from it. However, as one opens the gap, only part of the total flow energy is used to pull air though the test section, because now, there is a second inlet port to the tunnel. The remainder of the flow energy goes to pull air from the room into the gap. This air goes directly into the outlet section of the wind tunnel, bypassing the test section.

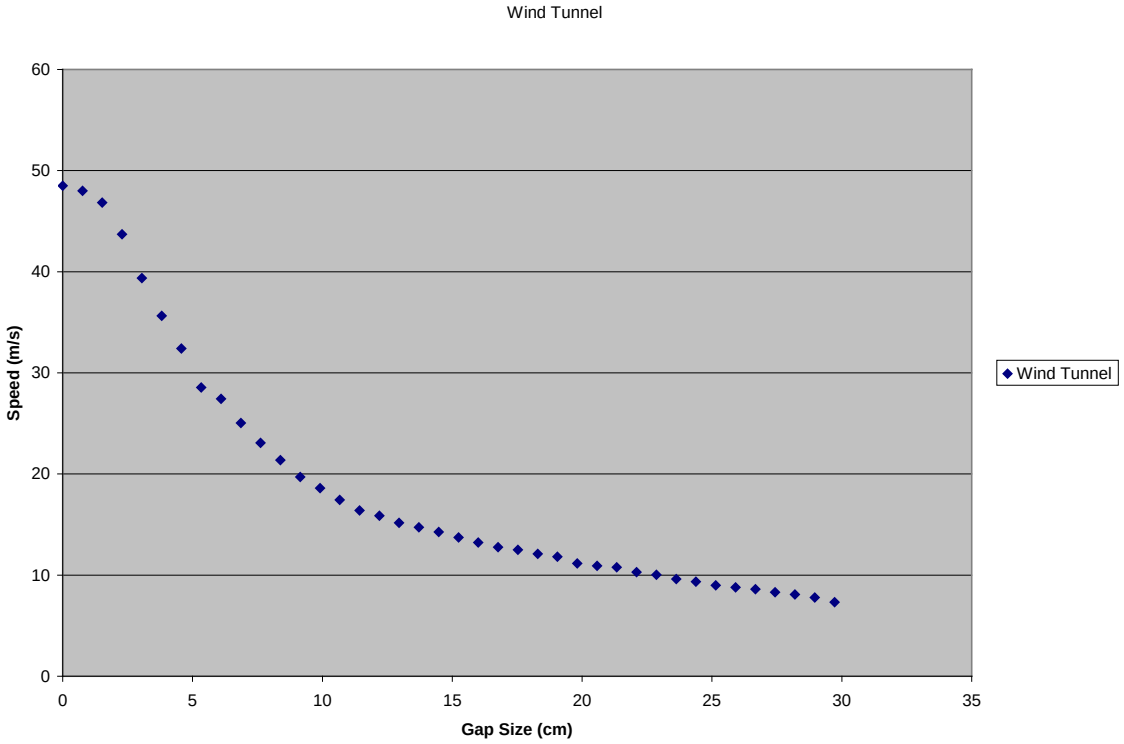

Figure 3: Calibration curve showing the air speed in the test section vs the width of the air gap.

EXPERIMENT 2: BOUNDARY-LAYER FLOW IN THE TEST SECTION

The purpose of this experiment is to demonstrate the existence of the boundary-layer in the test section of a wind tunnel. How this was achieved is explained below. For a given run, the speed of air at the centre of the test section is fixed. The pressure probe is moved to the geometric centre of the test section and the stagnation and static pressures are measured at that point. Then, the probe is moved to a series of predetermined points along the vertical line that go through the geometric centre. The stagnation and static pressures are measured at each such point. The pressure probe is moved vertically downwards in this way from its initial position all the way to the bottom wall of the test section, stopping as close to that wall as the thickness of the probe allows. By using small incremental displacements of the pressure probe and Equation (1) repeatedly, one determines the velocity profile along the chosen vertical line. In these experiments, small increments of 5 mm were used and found to be adequate, until one entered the boundary layer. Thereafter, increments of 1 mm were used. This process was repeated along three different vertical planes: the first plane was located one quarter of the way into the test section, following the direction of air flow ($L/4$); The second plane two-quarters of the way into the test section ($L/2$); and the third plane three-quarters of the way in ($3L/4$); where L is the length of the test section in the direction of flow. The speeds that were so determined are shown in Figure 4, where, due to symmetry about the horizontal plane, data are shown only for the bottom half of the test section.

The normalised height in Figure 4 refers to the height of the local point (at which velocity measurements were made) above the bottom plate divided by the height of the geometric centre of the test section above the same plate. Note that the geometric centre was the starting point for all measurements. In keeping with the tradition in boundary-layer theory, the horizontal axis portrays two different things simultaneously: position and velocity [6–9]. First, the numbers shown along the horizontal axis give the location (abscissas), measured relative to the leading edge of the plate, of the vertical plane (line) along which the velocity is being determined. Secondly, the magnitude of the normalised horizontal speed of fluid at each point along that vertical line are also represented horizontally using the (coloured) data points shown in that Figure. The normalised local speed in Figure 4 indicates the local speed of air at a given point divided by the speed of air at the geometric centre of the test section, which, again, was the starting point for all measurements.

It can be seen from Figure 4 that the speed of air in the test section remains constant as one moves vertically across the flow from the centre of the test section towards the bottom wall, until one reaches a certain critical distance from that wall. Thereafter, further downward movement of the probe yields speeds that decrease in magnitude continuously until one reaches the wall, where the speed of air must be zero, in conformity with the no-slip condition at the solid boundary

[6–9]. This behaviour is clearly demonstrated by each of the three plots shown in Figure 4. Naturally, the finite thickness of the probe did not allow us to get infinitely close to the wall. Therefore, expected boundary-layer behaviour can be observed along the first vertical plane ($L/4$), along the second vertical plane ($L/4$), and along the third vertical plane ($3L/4$). Furthermore, the thickness of the boundary layer increases in the direction of flow. This is qualitatively in agreement with how boundary layers behave theoretically, whether they be laminar, Equation (1), or turbulent, Equation (7) [6–9]. The background of the plot areas was darkened to heighten the contrasts of the colours chosen for the graphs.

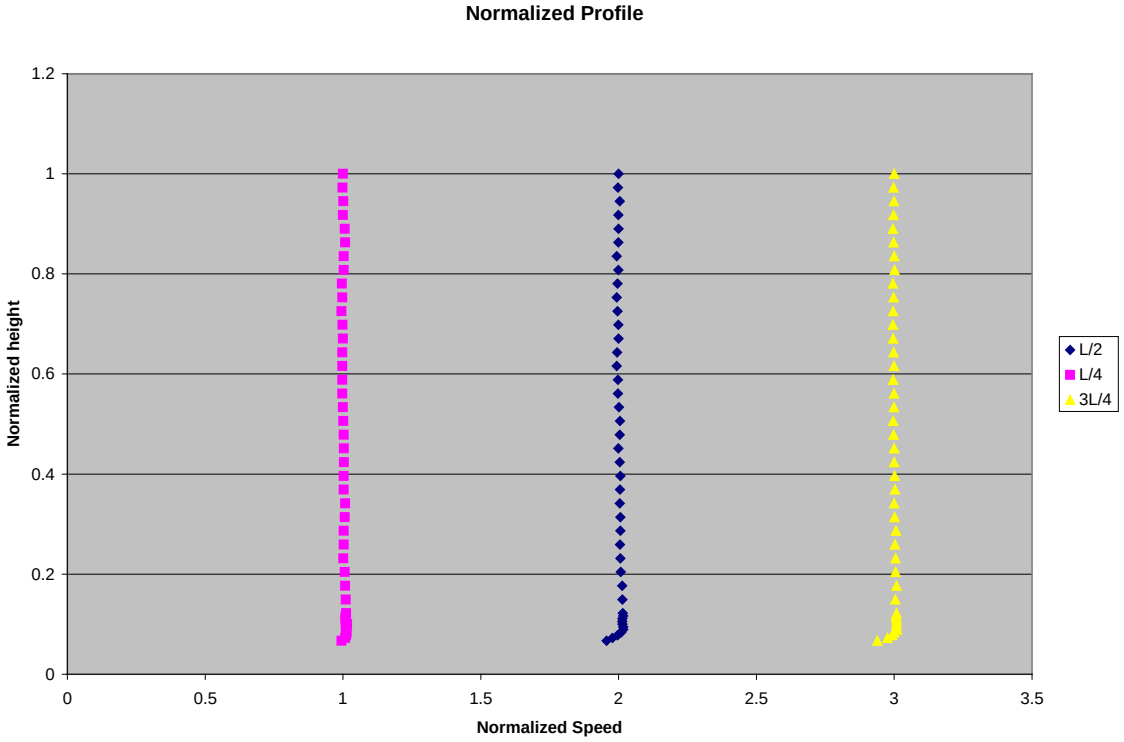

Figure 4: Velocity profiles at three different vertical planes in the test section ($L/4$, $L/2$, $3L/4$).

CHARACTERISATION OF BOUNDARY LAYERS

In order to characterise the boundary layer, that is, to determine whether it is laminar, transitional or turbulent, one needs to know the nature of the velocity profile inside the boundary layer. This information is rarely available, a priori. Traditionally, one proceeds by assuming a variety of velocity profiles, which is what was done in establishing Table 1 in this article and Table 9.2 of reference [2].

In boundary-layer theory, it is assumed that one knows where the origin of the coordinate system is, which is traditionally taken to be at the leading edge of the plate [6-9]. Here, however, an added complication is that it is not clear where the origin of the coordinate system should be. Three obvious choices for such an origin come to mind naturally: the inlet to the wind tunnel, the inlet to the test section, or somewhere between these two, such as where air exits the honeycomb-shaped strengtheners and begins to approach the test section directly. The corresponding distances in the wind tunnel are shown in Table 2.

Table 2: Three possible origins of the coordinate system.

Origin of the x-coordinate	x at $L/4$ (in)	x at $L/2$ (in)	x at $3L/4$ (in)
Inlet to the test section	6	12	18
Exit from the straighteners	48	54	60
Inlet to the wind tunnel	70	76	82

Each of these origins was tested and it was determined that placing the origin at the exit from the strengtheners was the best choice. This was because the other two possible origins yielded theoretical values of boundary-layer thicknesses that were either too small or too large compared to what was actually measured in the lab.

Using this chosen origin, the boundary layers were found to be turbulent and the workable power-law formulas had values of n between 6 and 7 [6-10]. This suggested fitting the data with curves obtained using multiples of the results for $n = 6$. By trial and error, the best results arose when the power law for $n = 6$ was multiplied by either 3 (denoted by $3n6$ in Figure 5) or by 5 (denoted by $5n6$ in Figure 5). The corresponding curves that show the growth of boundary-layers along the plate are in Figure 5.

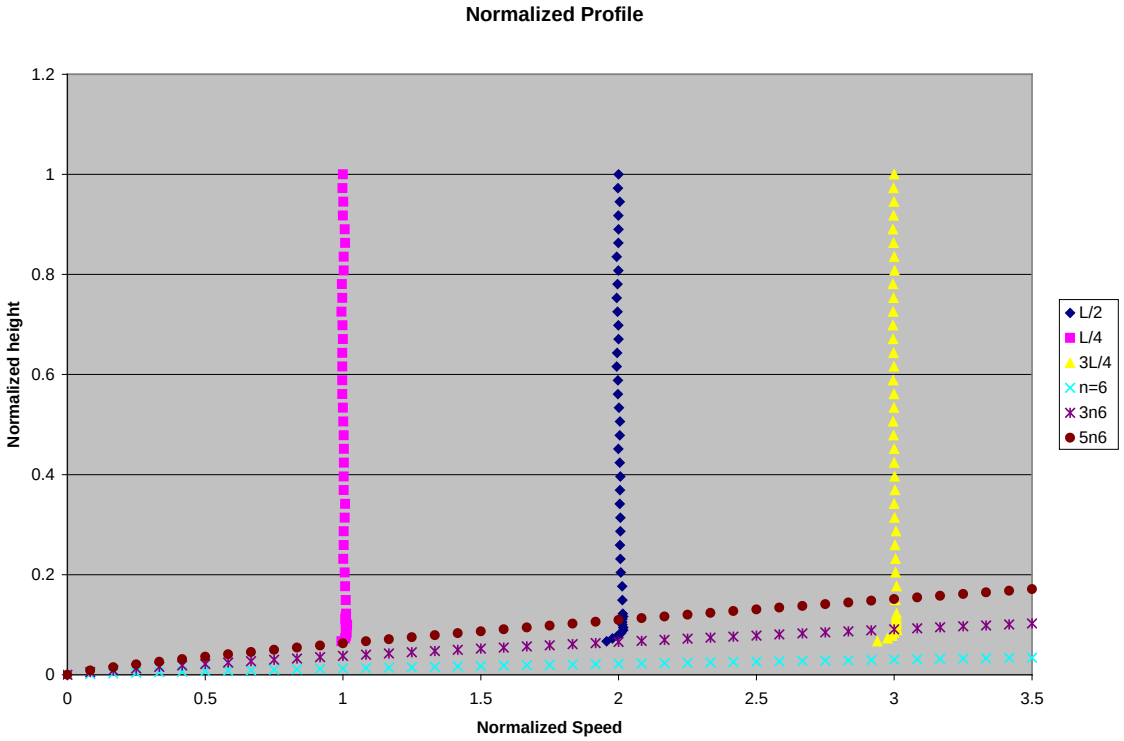

Figure 5: Normalised velocity profiles with superimposed curves for disturbance thicknesses, Equation (7). Note: *3n6* and *5n6* indicate that the curve for $n = 6$ had been multiplied by 3 and 5, respectively.

CONCLUSIONS

It is conventional to study boundary-layer flows in a wind tunnel by inserting and mounting a plate inside the test section. Such plates are both heavy and sharp-edged, which requires considerable care and alertness on the part of the students in order to prevent serious accidents. Two experiments presented in this article allow a class to study boundary layers over a flat plate experimentally by using the bottom wall of the test section as a built-in flat plate; no mounting or dismounting of plates is necessary in these experiments. The results obtained by students in our laboratory over many semesters agree qualitatively and quantitatively with those predicted by boundary-layer theory.

REFERENCES

1. Blasius, H., The boundary layers in fluids with little friction. *Zeitschrift fur Mathematik und Physik*, 56, **1**, 1–37 (1908) (in German). Note: English translation is available as NACA TM 1256, February (1950).
2. Fox, R.W., McDonald, A.T. and Pritchard, P.J., *Introduction to Fluid Mechanics*. (7th Edn), New York: John Wiley and Sons, 389-411 (2009).
3. Munson, B.R., Young, D.F. and Okiishi, T.H., *Fundamentals of Fluid Mechanics*. (5th Edn), Hoboken: John Wiley and Sons, 562-590 (2006).
4. Engineering Laboratory Design, Inc., Wind tunnels (2004), 15 March 2010, www.eldinc.com/wind/index.htm and www.eldinc.com/cgi-bin/StandardWindTunnel.pl?id=6
5. Njock Libii, J., Design of an experiment to test the effect of dimples on the magnitude of the drag force on a golf ball. *World Transactions on Engng. and Technol. Educ.*, 5, **3**, 478-480 (2006).
6. Faber, T.E., *Fluid Dynamics for Physicists*. Cambridge: Cambridge University Press, 240-251 (1995).
7. Batchelor, G.K., *An introduction to Fluid Dynamics*. Cambridge: Cambridge University Press, 302-324 (1967).
8. Schlichting, H., Boundary-Layer Theory. (7th Edn), translated by Kestin, J., New York: McGraw-Hill Book Company, 127-223 (1979).
9. Landau, L.D. and Lifshitz, E.M., *Fluid Mechanics. Vol. 6, Course of Theoretical Physics*. Translated by Sykes, J.B. and Reid, W.H., London: Pergamon Press, 157–189 (1959).
10. Moin, P. and Kim, J., Tackling turbulence with supercomputers. *Scientific American*, January, 62-68 (1997).